89th AMS Annual Meeting, 16th Conference on Satellite Meteorology and Oceanography, 11-16 January 2009, Phoenix, AZ.

JP6.5 MICROPHYSICS SCHEMES BASED ON DSD-PARAMETER CONSTRAINTS AND THEIR IMPACT ON CONVECTIVE STORM FORECASTS

Charlotte E. Wainwright*[1], Ming Xue[1,2], Guifu Zhang[1,2], and Daniel T. Dawson[1, 2]
[1]*School of Meteorology, University of Oklahoma, Norman, OK*
[2]*Center for Analysis and Prediction of Storms, Norman, OK*

1. INTRODUCTION AND MOTIVATION

It is clear that in order to accurately model convective scale events, we require the most accurate microphysical schemes possible. However this need for detailed microphysical parameterization must be balanced with the computational expense that such detailed parameterizations require.

A new way of calculating the drop-size distribution (DSD) parameters in the single moment (hereafter SM) and double moment (hereafter DM) microphysical scheme available in the Advanced Regional Prediction System (ARPS; Xue et al. 2003) has been implemented and is tested here using the ARPS test case of the May 20, 1977 Del City, Oklahoma tornadic supercell storm. This case has been examined in detail many times previously using a variety of platforms.

Recent work by Zhang et al. (2008) used a method of deriving relationships between the moments of the gamma DSD in order to develop a diagnostic relation between the intercept parameter and the water content. The relationships that they derived were based on Two-Dimensional Video Disdrometer (2DVD) measurements taken in Oklahoma during the summer seasons of 2005, 2006 and 2007. These data are expected to be representative of the kind of severe convective events that are often witnessed in the Southern Great Plains region. Further work needs to be done to establish whether these derived moment relations are valid for other areas and types of rainfall event. It is well known that the DSD parameters can vary significantly between stratiform and convective events (e.g. Tokay et al. 1995) and Munchak and Tokay (2008) found that the shape parameter of the gamma DSD varies regionally. This reinforces the need to move towards a tunable DSD parameter model, since modeling the governing parameters as constants is clearly making an approximation without good physical basis. It can also be seen in multi-moment model simulations that the DSD parameters can vary widely within a single storm. For example, we get very large drops on the leading edge of strong convective events, as has been witnessed observationally. Model simulations of the May 3rd 1999 tornadic supercell event performed using the Advanced Regional Prediction System (ARPS, Xue et al. 2003) and the Milbrandt and Yau (2005b) three-moment microphysics scheme illustrate this variation of the DSD parameters within the storm (Dawson et al. 2008). Figure 1 shows the variation of the gamma DSD shape parameter α across the domain one hour into the simulation at 277 m height. It is clear that the shape parameter varies widely across the storm domain. This again reinforces the need for appropriately complex microphysics options, as the assumption of a constant shape parameter (as in the exponential DSD) clearly cannot capture the full complexity of the DSD, which will have impacts for many microphysical processes.

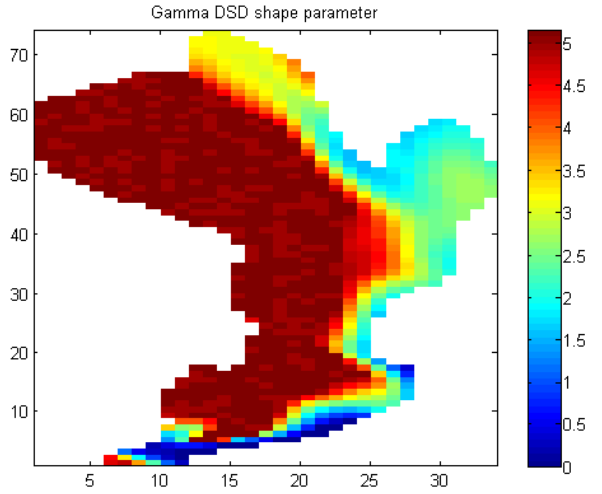

Fig. 1. The variation of the shape parameter of the gamma droplet size distribution across the storm domain.

In this paper we discuss the derivation and implementation of a diagnostic relation between DSD parameters within the single- and double-moment microphysical schemes in the three-dimensional non-hydrostatic ARPS model. The derived relationships are compared to those derived from observational disdrometer measurements. Simulations of a severe tornadic convective event performed using the newly implemented diagnostic DSD based microphysics schemes are discussed with regard to the impact of the microphysical schemes on the resulting analysis and in comparison to simulations performed using the original single-, double- and triple-moment schemes.

2. SIMULATIONS

The case tested is the 20 May 1977 convective event, which is the default test case of the ARPS model. On this day there were sixteen tornadoes across Oklahoma. The case studied here produced a tornado in Del City. The synoptic setup on this day was conducive to severe, long-lasting storms; an occluded front extended across the Western Oklahoma panhandle with a cold air boundary extending south-west across the state due to nocturnal thunderstorms. Strong vertical wind shear across central Oklahoma and south-easterly low-level flow brought warm, moist air into the unstable air mass and a shortwave at 500mb approaching from the south-west added to the instability (Ray et al. 1980).

Several simulations of the 20 May 1977 convective event were performed using the ARPS. The model contains a variety of microphysics scheme options, including single-, double- and triple-moment schemes. A 'truth' simulation was first performed using the Milbrandt and Yau triple-moment scheme (Milbrandt and Yau 2005a, Milbrandt and Yau 2005b), hereafter MY3, altered slightly to allow negative values of the shape parameter to be included as this was previously limited by a minimum of zero, and it has been seen that negative values of the shape parameter of the gamma DSD are possible. Each simulation was performed at the same 1 km horizontal resolution with 67 vertical levels and using the same time-step to allow for direct comparison.

Further simulations were performed using the single-moment and double-moment Milbrandt and Yau schemes (hereafter MY1 and MY2 respectively). The single- and double- moment schemes were then modified to include the derived DSD-parameter relations. The single-moment scheme was altered to include the diagnostic relation between the water content and the intercept parameter of the DSD, as derived from the moment relations found from triple-moment model output data. The modified double-moment scheme includes both this relation and a direct relation between the shape and slope parameters of the gamma DSD. Zhang et al. (2001) first examined the link between these two DSD parameters and derived a polynomial relation between the shape and slope parameters using disdrometer data collected in east-central Florida during the summer of 1998. Although the coefficients of the relation have changed slightly since then based on new observations, the strong relation between the shape and slope parameters has been shown to be robust.

The DSD parameter and moment relations derived by Zhang et al (2008) were derived using 2DVD measurements encompassing summer rainfall events over Oklahoma. These are compared with relations utilized here which were derived from model output data. The triple-moment model output data used was from an ARPS model simulation of the May 3rd 1999 tornadic supercell that struck central Oklahoma. It was hoped that the relations derived from the model output would be similar to those derived from the 2DVD data, since the May 3rd event was a severe convective event, and it is known that the majority of the rainfall events that comprise the 2DVD measurements will be convective events of varying severity.

3. DERIVED DSD-PARAMETER RELATIONS

The method used to derive the DSD parameter relations follows the moment relation method (MRM) of Zhang et al. (2008). Recall that the n^{th} moment of the exponential distribution is given by

$$M_n = \int D_n N(D) dD = N_0 \Lambda^{-(n+1)} \Gamma(n+1) \qquad (1)$$

Such that Λ and N_0 can both be determined from any pair of moments of the DSD.

In the moment relation method, the first step is to establish a power law relationship between two moments of the DSD. Once this has been established, it can be used to reduce the exponential distribution to a single free parameter and then the number concentration N_0 can be determined from the water content W. Making use of the relation between the water content and the third moment of the DSD we can find the water content in terms of the DSD parameters

$$W = \rho \pi N_0 \Lambda^{-4} \qquad (2)$$

By substituting (1) into the power law moment relation and making use of the relation for Λ found by rearranging (2) we can find a power law relation between the number concentration and the water content

$$N_0 = \alpha W^{\beta} \qquad (3)$$

where α and β depend on the coefficients and order of the moment pair used to determine the power law relation as well as the water density. Details and formulae for α and β can be found in Zhang et al. (2008).

There are several options for which moment pairs to use to derive the $N_0 - W$ relation. Cao et al. (2008) assessed the relative errors of the DSD moments gained from 2DVD data after error reduction via sorting and averaging based on two parameters. They found that the middle moments (M_2, M_3 and M_4) have a much lower relative error compared to M_0 and M_6. The lowest moments are also more affected by the limited area of the disdrometer compared to the higher moments. For these reasons, the middle moment pair (M_2, M_4) is used for DSD fitting since their results should provide a more robust and reliable relation. The relation for this moment pair gained from the disdrometer measurements was $M_2 = 1.42\ M_4^{0.836}$.

A comparable relation was derived using ARPS model output for the May 3rd 1999 storm. The simulation was performed using the Milbrandt and Yau triple moment microphysics scheme (MY3) and initial conditions were produced using the a sounding extracted from the ARPS Data Analysis System (ADAS). The output data used to derive this relation was that from the surface level of the model, in order to be able to make direct comparisons with the measured disdrometer data, which is representative of the observed DSDs at the surface only.

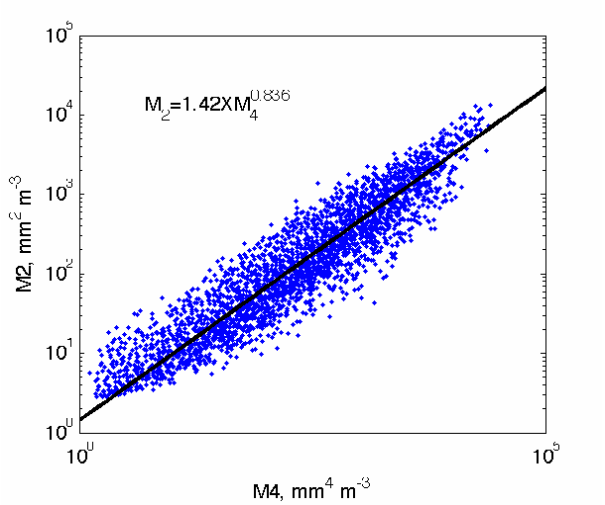

Fig. 2. Second and fourth moment relation from 2DVD measurements taken over three Oklahoma summer seasons (taken from Dawson et al. 2007)

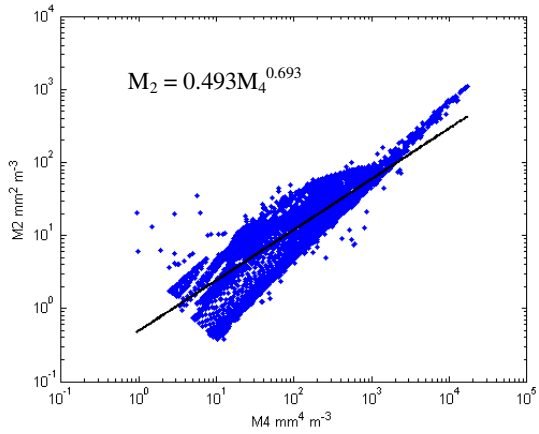

Fig. 3. Second and fourth moment relation from model simulation output of the May 3rd 1999 Oklahoma tornadic supercell storm.

Examination of Figs. 2 and 3 reveals a very similar trend between the data from the two different sources. The moments from both data sources cover a similar range of values, and the power law trend seen is rather similar between the two figures, as the power law derived from the model output is $M_2 = 0.493M_4^{0.693}$. This is reasonably close to that derived from the disdrometer measurements when we consider that the disdrometer measurements cover a large number of events. Whilst the range of disdrometer measurements mainly encompasses convective events, there will be a number of different rainfall types covered within the dataset, as the disdrometer will also have measured stratiform rainfall as well as severe convective events such as that from which the model output is taken. This is one of the reasons why we see more scatter in Fig. 2 than Fig. 3, as Fig. 3 is representative of only one single convective event.

Using the formulae of the moment relation method described in Zhang et al. (2008), the observationally derived relation translated into a relation between the water content and the DSD number concentration of $N_0(M_2,M_4) = 7106W^{0.648}$. Following the same procedure as outlined in their paper, using the surface level model simulation output data, we find a relation of $N_0(M_2,M_4) = 0.075W^{0.275}$. The diagnostic N_0 relation was used to modify the single-moment (MY1) microphysics scheme. The double moment scheme was extended to include both this relation and a relation between the shape and slope parameters. The relation between gamma DSD parameters is illustrated in Figure 4.

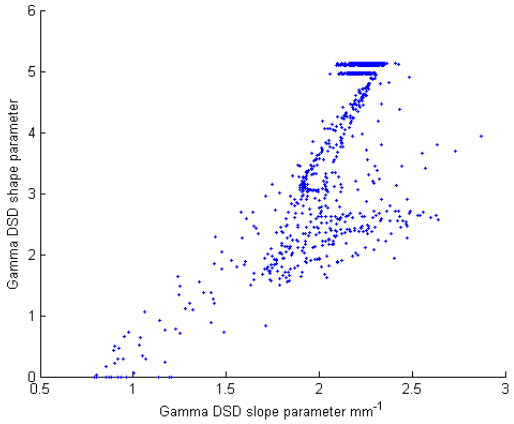

Fig. 4. Scatter plot showing the relation between the gamma DSD shape and slope parameters, taken from model simulation output of the May 3rd 1999 Oklahoma tornadic supercell storm.

A diagnostic relation between the two parameters was also added to the modified double-moment microphysics scheme, allowing us to effectively create a double-moment microphysics scheme with diagnostic alpha. The results from simulations performed using this and the modified single-moment scheme are discussed in the following section.

4. MODEL SIMULATION RESULTS

We now examine the results of the ARPS simulations of the May 20th 1977 Del City tornadic

supercell with reference to the effect of the diagnostic microphysics scheme.

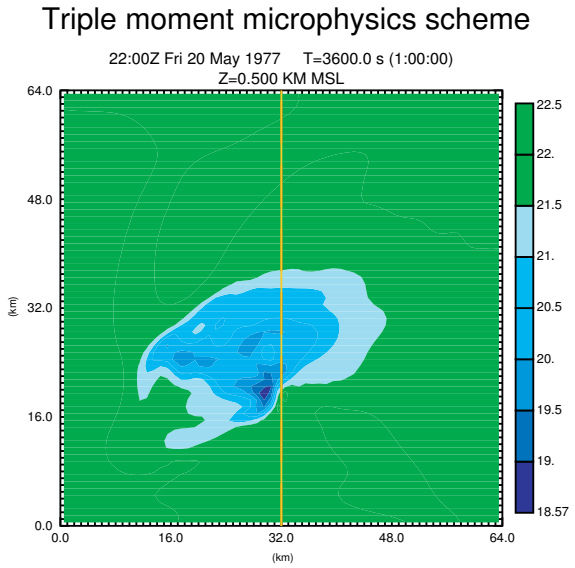

Fig. 5. Temperature at 0.5km height and 3600 seconds from the triple moment ('truth') simulation.

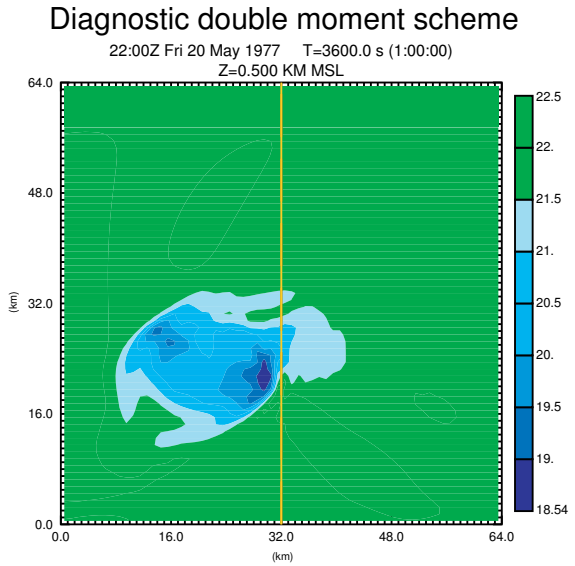

Fig. 6. Temperature at 0.5km height and 3600 seconds from the diagnostic double moment simulation.

Examination of Figs. 5 and 6 shows that one hour into the simulation, the diagnostic double moment scheme is producing very similar results for the temperature field to the triple moment scheme (which we are using as the 'truth' simulation here). It is typical for lower-moment microphysical schemes to over-estimate the strength of the cold pool, however the cold pool is seen to be very close in strength and location in the two figures. We can also compare the results to those from the original double-moment scheme (not shown). The original double-moment scheme extended the boundary of the coldpool further to the north-east then the diagnostic scheme, although the original double-moment scheme also has an enhanced coldpool to the west of the main coldpool which is not seen in either the diagnostic double-moment or triple moment output. This is encouraging, since it has been seen that at resolutions of 1 km or less, the microphysics has a large impact on the cold pool and reflectivity structure (Dawson et al. 2008), and cold pool structure is known to be important for tornadic potential.

We can also compare the reflectivity structure from the two schemes, shown in Figs. 7 and 8. Examination of these figures shows that the overall reflectivity structure is again similar between the two schemes, although there are some differences. The finger of low reflectivity close to the center of the domain is clearly witnessed in both of the simulations, but the diagnostic double-moment scheme extends an area of higher reflectivity between the two separate areas of high reflectivity seen in Fig. 7, and the area of highest reflectivity extends further west than that seen in the triple-moment simulation. The diagnostic double-moment scheme also has some areas of higher reflectivity in the South-East which are not witnessed in the truth simulation.

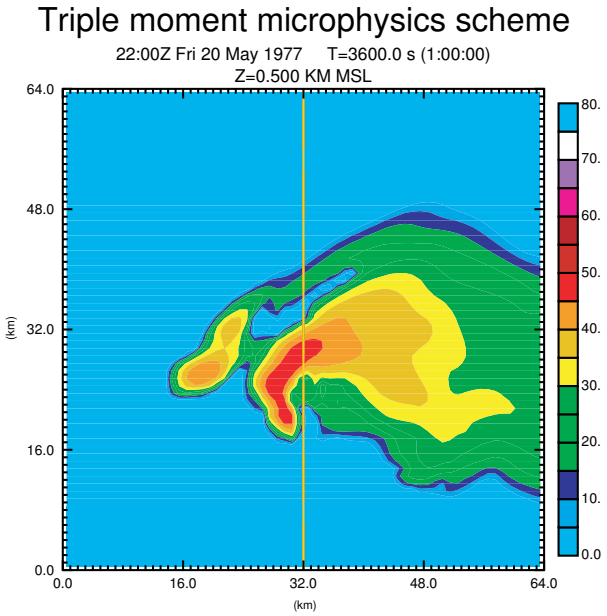

Fig. 7. Reflectivity in dBZ at 0.5km height and 3600 seconds from the triple moment ('truth') simulation.

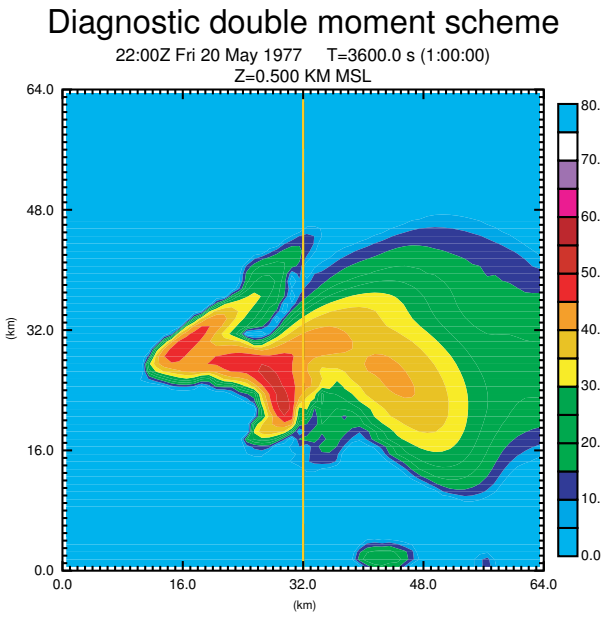

Fig. 8. Reflectivity in dBZ at 0.5km height and 3600 seconds from the diagnostic double moment simulation.

Figures 9,10 and 11 show the total water content in g kg^{-1} for the 'truth', diagnostic double-moment and original double-moment simulations. Again it is clear that the overall structure of the water content is similar, with the areas of highest water content in the same location. The region of higher water content extends farther westward in the diagnostic double moment scheme. The original double-moment scheme places the enhanced moisture region in the same location but it is

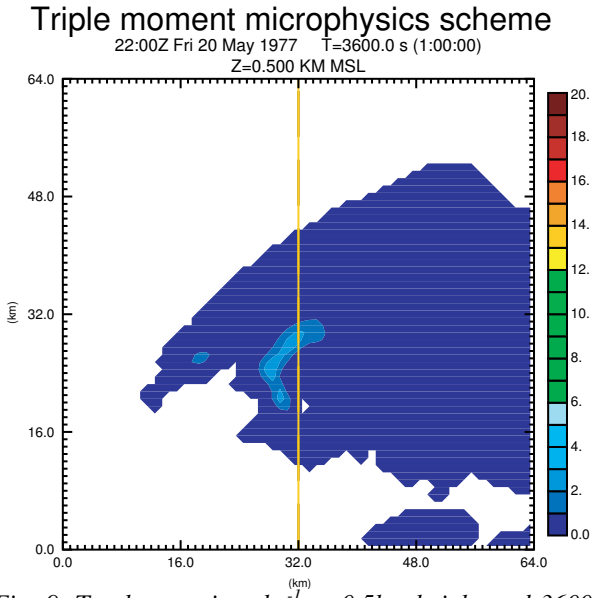

Fig. 9. Total water in g kg^{-1} at 0.5km height and 3600 seconds from the triple moment ('truth') simulation.

smaller and weaker. However the original double-moment scheme did not predict the water content in the southwest of the domain which is seen in both the diagnostic double-moment and the triple moment schemes. Since the diagnostic scheme bases the number concentration on the water content, this explains the presence of enhanced reflectivity in this area in the diagnostic double-moment scheme.

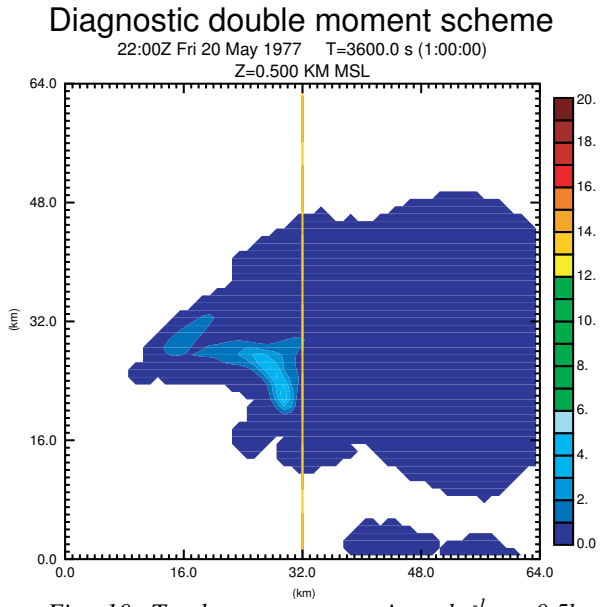

Fig. 10. Total water content in g kg^{-1} at 0.5km height and 3600 seconds from the diagnostic double moment simulation.

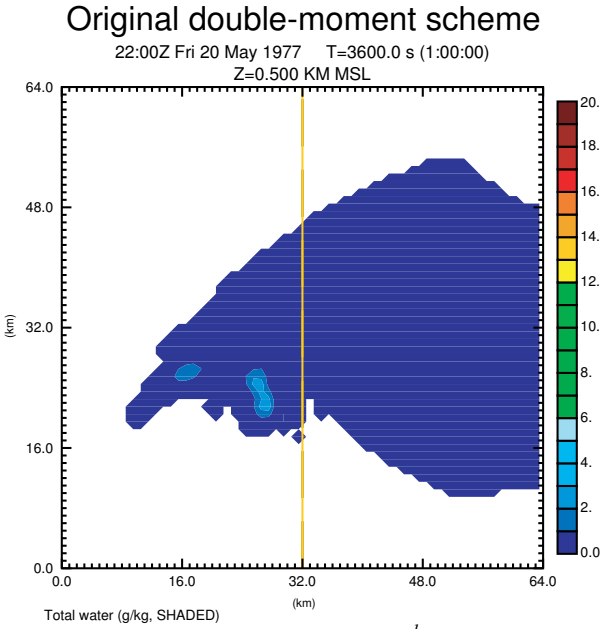

Fig. 11. Total water content in g kg^{-1} at 0.5km height and 3600 seconds from the original double moment simulation.

All of the results discussed so far have been at 0.5 km height above mean sea level. As the height

increases, the results of the diagnostic double-moment scheme are seen to deviate from those of the triple moment scheme and the results are closer to those of the original double-moment scheme. This is to be expected, because as the height increases, a larger proportion of the hydrometeors are going to be part of the frozen hydrometeor classes, and the diagnostic relation was only applied to the warm rain microphysics. Extension to other hydrometeor categories or the use height-dependent coefficients in the diagnostic N_0 relation are two possible ways to remedy this that will be investigated.

The results of the diagnostic double-moment scheme so far are encouraging, as it produces results similar to those produced using the triple moment microphysics scheme with less computational expense. Further work needs to be done to extend the relations to other hydrometeor types and ice processes.

5. SUMMARY AND FUTURE WORK

A new DSD-parameter relation based diagnostic microphysics scheme has been implemented in the ARPS model based on the Milbrandt-Yau multi-moment scheme. It is clear from the model output that the diagnostic relation based microphysics scheme performs well at lower levels but loses its benefit at higher heights. This is as expected, as the relation has only been implemented in the warm rain microphysics scheme. Results so far from the diagnostic double-moment scheme are encouraging. This illustrates that the use of the moment relation method (Zhang et al., 2008) to derive DSD parameter relations produces realistic relationships, and that the use of diagnostic relations between DSD parameters can provide significant benefits to lower-moment microphysics schemes without greatly increasing the computational cost.

Future plans involve examining DSD parameter relations for other hydrometeor types and extending the implementation of the DSD-based microphysics scheme to other hydrometeor types. It is expected that this will have a beneficial impact on the results at higher levels. This will hopefully allow us to gain results that are closer to a three moment scheme whilst retaining a similar level of computational expense to a double-moment scheme.

Other future plans are to extend the diagnostic relations to be dependent on height or perhaps temperature, as it is known that the relationship between the DSD parameters alters within different levels of the storm. This was witnessed in the model output used to derive the implemented relations here, but further cases will need to be examined to confirm the robustness of this height dependence, since observational DSD data at different height levels and for different hydrometeor types is more sparse than surface data. One way to achieve this may be to make use of DSD retrieval from dual-polarimetric Doppler radar data.

We also plan to test the DSD-parameter constraint based microphysics schemes on other cases, including cases for different rain types such as stratiform rain. The data set from which the DSD-parameter relations were derived will also be extended with more model output data and observational data, and the relations modified as necessary.

Acknowledgement: This work was primarily supported by NSF grant ATM-0608168.

REFERENCES

Cao, Q., G. Zhang, E. Brandes, T. Schuur, A. Ryzhkov and K. Ikeda, 2008: Analysis of Video Disdrometer and Polarimetric Radar Data to Characterize Rain Microphysics in Oklahoma. *J. Appl. Meteor. Climat.,* **47,** 2238-2255.

Dawson, D. T., M. Xue, J. A. Milbrandt, M. K. Yau and G. Zhang, 2007: Impact of multi-moment microphysics and model resolution on predicted cold pool ad reflectivity intensity and structures in the Oklahoma tornadic supercell storms of 3 May 1999. Preprints, *18th Conf. on Numerical Weather Prediction*, Park City, UT, Amer. Meteor. Soc.

Dawson, D. T., II, M. Xue, J. A. Milbrandt, and M. K. Yau, 2008: Improvements in the treatment of evaporation and melting in multi-moment versus single-moment bulk microphysics: results from numerical simulations of the 3 May 1999 Oklahoma tornadic storms. *24th Conf. Severe Local Storms*, Savannah, GA, Amer. Meteor. Soc., Paper 17B.4.

Milbrandt, J. A. and M. K. Yau, 2005a: A multi-moment bulk microphysics parameterization. Part I: Analysis of the role of the role of the spectral shape parameter. *J. Atmos. Sci.,* **62,** 3051-3064.

Milbrandt, J. A. and M. K. Yau, 2005b: Part II: A proposed three-moment closure and scheme description. *J. Atmos. Sci.,* **62,** 3065-3081.

Munchak, S. J. and A. Tokay, 2008: Retrieval of raindrop size distribution from simulated dual-frequency radar measurements. *J. Appl. Meteor. Climat.,* **47,** 223-239.

Ray, P. S., B. C. Johnson, K. W. Johnson, J. S. Bradberry, J. J. Stephens, K. K. Wagner, R. B. Wilhelmson, and J. B Klemp, 1980: The morphology of several tornadic storms on 20 May 1977. *J. Atmos. Sci.,* **38,** 1643-1663.

Tokay A., and D. A. Short, 1996: Evidence from tropical raindrop spectra of the origin of rain from

stratiform versus convective clouds. *J. Appl. Meteor.*, **35**, 355–371

Xue, M., D.-H. Wang, J.-D. Gao, K. Brewster, and K.K. Droegemeier, 2003: The Advanced Regional Prediction System (ARPS), storm-scale numerical weather prediction and data assimilation. *Meteor. Atmos. Physics*, **82**, 139-170.

Zhang, G. J. Vivekanandan and E. A. Brandes, 2001: A method for estimating rainrate and drop size distribution from polarimetric radar measurements. *IEEE Trans. Geosci. Remote Sens.,* **39,** 830-841.

Zhang, G., M. Xue, Q. Cao and D. Dawson, 2008: Diagnosing the Intercept Parameter for Exponential Raindrop Size Distribution Based on Video Disdrometer Observations: Model Development. *J. Appl. Met and Climat.*